Annals of Science and Inquiry
Vol. 2 No. 6 (2026)

Correlation depends on the coordinates: paired range-bearing residuals in a three-observer MR.CLAM record

Aaron Crawford[1] · Timothy Murphy[2] · Jason Reed[3]

[1] Croatia · [2] Greece · [3] Romania

Published: June 17, 2026 | Article 848

Abstract

The same two-dimensional discrepancy can have different component correlations when expressed forward/left or along/across a target sightline. In released MR.CLAM camera records, we reconstructed supported references for 9,042 landmark and 1,163 robot observations. Body and line-of-sight Pearson correlations were -0.247 and 0.134 for landmarks, but 0.790 and -0.871 for robots. The robot contrast crossed zero when entire observers or targets were omitted, and rank correlations gave a different account of association. Seven records with assigned targets behind the observer remained in the analysis. Coordinate rotation is a mathematical fact; these empirical magnitudes describe the particular angular and target composition of the release. They do not isolate intrinsic camera noise or demonstrate calibration or controller improvement. Keywords: range-bearing observations; relative position; covariance; line of sight; source reference; cooperative localization

Correlation depends on the coordinates: paired range-bearing residuals in a three-observer MR.CLAM record

Abstract

The same two-dimensional discrepancy can have different component correlations when expressed forward/left or along/across a target sightline. In released MR.CLAM camera records, we reconstructed supported references for 9,042 landmark and 1,163 robot observations. Body and line-of-sight Pearson correlations were -0.247 and 0.134 for landmarks, but 0.790 and -0.871 for robots. The robot contrast crossed zero when entire observers or targets were omitted, and rank correlations gave a different account of association. Seven records with assigned targets behind the observer remained in the analysis. Coordinate rotation is a mathematical fact; these empirical magnitudes describe the particular angular and target composition of the release. They do not isolate intrinsic camera noise or demonstrate calibration or controller improvement.

Keywords: range-bearing observations; relative position; covariance; line of sight; source reference; cooperative localization

1. From a polar observation to a state coordinate

A monocular detection of a barcode can provide both range and bearing. Reconstructing a relative position from that pair is straightforward algebraically, yet the meaning of its component correlation is less straightforward. A residual described as forward and left is expressed in the observing robot's body axes. The same residual described as along and across the target sightline uses axes that vary with the target direction. A strong correlation in one representation need not imply equally strong dependence in the other. The issue concerns what is being summarized, before considering whether a state estimator or controller could use the information effectively.

Probabilistic robotics separates a sensor observation model from the latent state to which it relates (Thrun et al., 2005). Coordinate frames and transformations are equally explicit in robotic state estimation (Barfoot, 2017) and robot kinematics (Lynch and Park, 2017). These distinctions matter when connecting observations to a multiagent state description. Xu et al. (2023), for example, define planar position and heading within their fixed-wing formation state and assemble individual states into a system vector. That is relevant context for specifying which coordinates represent information. The present study concerns physical ground-robot camera observations; it does not implement that policy, infer its sensor model, or assess aircraft formation performance.

There is established work on converting polar observations and their uncertainty. Lerro and Bar-Shalom (1993) study debiased converted measurements in tracking, while Bar-Shalom et al. (2001) treat estimation and measurement models in tracking and navigation. Nonlinear transformations of moments are addressed by Julier et al. (2000), and Julier and Uhlmann (2004) review the unscented transformation for propagating mean and covariance information. Our analysis does not introduce a new conversion algorithm or use a filtering approximation. It transforms each released observation directly, then describes the residual pairs actually obtained.

The UTIAS dataset was designed for cooperative localization and mapping, with camera observations and motion-capture references (Leung et al., 2011). Subsequent research has examined cooperative localization under changing sensor qualities and communication rates (Sullivan et al., 2018). Thus neither the importance of sensing quality nor the possibility of range/bearing dependence is new. Our narrower research question is: **how do joint residual relationships differ between body and line-of-sight**

coordinates on the same supported observations, overall and within fixed reference-bearing bands? Static-landmark and moving-robot targets are analyzed separately.

Two propositions organize the comparison. P1 is a coordinate identity: rotating a residual into the sightline axes preserves its length for each observation. P2 is an empirical question: the pooled and stratified component associations may differ under those representations because their axes and recorded target composition differ. We estimate the actual associations and their finite composition sensitivity. No directional causal effect of bearing, physical noise mechanism, independence assumption, or gain from changing a controller is identified by these propositions.

2. What the available archive actually contains

We reuse eight complete numeric members of MR.CLAM dataset 6: the barcode map, all static-landmark references, and groundtruth/measurement files for observers 1-3. Their extracted size is 9,759,639 bytes. They are contained in an already acquired 2,377,645-byte prefix of the official 3,966,584-byte archive. Each needed member was decompressed again from its local ZIP header, checked against its CRC32, compared byte-for-byte with the extracted file, and matched to its recorded SHA256. The full archive and its central-directory checksum are unavailable; individual-member integrity is the scope of verification. Selection follows available complete archive members, rather than a choice of favorable residuals. Observations from all five robots are not claimed.

The three measurement files contain 1,942, 4,031 and 5,627 rows, respectively. Every row records timestamp, encoded identifier, range in meters and bearing in radians. Range and bearing therefore refer to the same detection event. All values are finite, and every recorded range is positive. Repeated timestamps with different targets are retained as separate detections. There are no duplicated or conflicting observer-timestamp-barcode groups. These rows are observations within a collection, not 11,600 independent experiments.

Identifier interpretation requires more than reading a column header. The raw measurement header labels its identifier as a subject number, but values include codes such as 90. The official loader names this value barcode_num, and the accompanying animation looks it up in the barcode map (Autonomous Space Robotics Lab, n.d.). The map is bijective across 20 subjects: robots 1-5 and landmarks 6-20. For instance, raw barcode 14 maps to robot subject 2; landmark subject 14 has barcode 61. Treating those two notions of identity as interchangeable would create a geometrically different reference.

Three rows have unmapped codes: observer 1 raw row 1094 has 43, and observer 3 rows 3754 and 3758 have 34. We retain their raw measurements and leave derived reference residuals missing. We do not infer a replacement target from whichever position happens to fit. This illustrates why data quality includes interpretability and contextual meaning, as well as numerical accuracy (Wang and Strong, 1996). Dataset documentation about collection, composition and permitted uses is likewise necessary for reuse (Gebru et al., 2021). Neither an integer-valued identifier nor a finite range guarantees that an observation has a supported correspondence.

The source places the camera and robot body frames at the same planar origin and orientation, with their displacement confined to the vertical direction. Its animation constructs a world endpoint using range times cosine or sine of bearing plus heading. We read those author scripts as inert text and did not execute them. The released robot pose contains x, y and heading in the Vicon inertial frame; static landmark positions are averaged Vicon coordinates with reported x/y standard deviations. These facts support a planar reference without fitting an empirical sign, rotation offset, lever arm or clock adjustment.

Reference information remains uncertain. The authors describe positional accuracy of roughly one millimeter in their workspace and report NTP timing errors of approximately one millisecond on average and ten milliseconds at maximum. We treat these as producer statements. Per-event orientation uncertainty is not supplied, and clock or correspondence error can enter the residual alongside camera error. Measurement-uncertainty guidance distinguishes a stated measurand and uncertainty model from an assertion of exact truth (Joint Committee for Guides in Metrology, 2008). Its multivariate supplement explicitly considers joint output quantities and coordinate transformations (Joint Committee for Guides in Metrology, 2011). Our empirical covariance matrices are descriptions of measurement-minus-source-reference discrepancies, not a certified uncertainty budget.

3. Fixed support and paired residual model

The protocol was frozen after schema inspection, timestamp and association checks, and nine nonrandom geometry examples. Those examples were the first three supported landmark observations per observer; they were not a prevalence sample. Complete-file covariances, correlations and group deletions were calculated afterward. All original rows remain in the processed table, including unmapped targets, unavailable target groundtruth and failed time support.

Every serialized measurement and robot-reference timestamp has three decimal places. We parse the text into integer milliseconds, preserving its original value rather than rounding onto a new common grid. This avoids subtractive rounding when comparing large floating-point timestamps at a 50-millisecond limit. Floating-point representation and numerical stability are separate from measurement accuracy (Goldberg, 1991; Higham, 2002). Three stored decimal places do not establish three-decimal-place clock accuracy.

At an observation time, a pose is supported if its native timestamp is exact or if neighboring native rows bracket it with a total gap no larger than 50 integer milliseconds. There is no extrapolation. Position is interpolated linearly, and heading uses the shortest circular arc. Actual median reference spacing is about 16 milliseconds, with gaps reaching 334 milliseconds, so nominal sampling frequency cannot substitute for this check. A moving target requires its own supported pose; a static landmark uses its recorded mean position. No residual magnitude determines inclusion. Integer-clock eligibility matched the earlier floating-clock source gate for every row.

Let p and theta denote the supported observer position and heading, and let l be the target position. The source-reference vector in body coordinates is

$$q^* = R(-\theta)(l - p), \quad r^* = \|q^*\|_2, \quad \varphi^* = \operatorname{atan2}(q_y^*, q_x^*).$$

For the observed pair (r,phi), define er=r-r$*$ and ea=wrap(phi-phi$*$), where wrap(a)=atan2(sin(a),cos(a)). We retain the returned signed principal angle, including the endpoint sign if an exact pi occurs. Directional-data methods require this periodic geometry to be explicit (Mardia and Jupp, 1999; Fisher, 1993). Our Pearson coefficient involving ea is a linear correlation of that wrapped residual, not a circular-linear correlation coefficient or a test that disregards the angular branch.

The body residual and sightline residual are

$$e_b = (r\cos\varphi, r\sin\varphi)^T - q^*,$$
$$e_{parallel} = r\cos(e_a) - r^*, \quad e_{perp} = r\sin(e_a).$$

They satisfy eb=R(phi$*$)[e_parallel,e_perp] and equal squared lengths. Both representations therefore use identical range, bearing, target and reference records. Because phi$*$ varies across observations, their pooled centered covariance matrices need not be related by one common rotation. Their mean vectors can

differ too. Pointwise length invariance does not require equality of pooled correlation or of the trace of a centered covariance matrix.

Within each declared subset, we report the centered sample covariance with denominator N-1 and Pearson correlation for three pairs: range/angular residual, body x/y residual and along/across residual. Pearson's standardized cross-moment summarizes linear association (Pearson, 1896). Rank association is reported separately using Spearman correlation (Spearman, 1904), with average ranks for ties, whose treatment matters in ranking problems (Kendall, 1945). The primary contrast is Delta r=r_body-r_LOS. Its possible range is [-2,2], although each correlation lies in [-1,1]. An undefined coefficient would remain missing whenever N<3 or a component had zero variance.

Target classes are never combined into a single headline correlation. Within each class, supported events receive equal weight, retaining unequal observer and target frequencies. We report class totals, each observer, and fixed reference-bearing bands: left below-0.20 rad, center from-0.20 through 0.20 rad inclusive, and right above0.20 rad. The outer bands are unbounded; they are not visibility tests. Reference bearing is used so that the noisy measured bearing does not itself define the stratum. The bands describe support and geometry, not randomized angular treatments.

The predeclared composition checks omit each of three observers in turn and, separately, each represented target. There are 15 landmark-target deletions and three robot-target deletions. Each recomputes the class coefficients and their contrast, retaining the entire remaining data. Their minimum and maximum form deterministic deletion ranges, not confidence intervals, independent-run variability or probability coverage. Robust statistics and influence analysis explain why dependence on a small part of a record deserves examination (Huber and Ronchetti, 2009; Hampel, 1974), but we fit no robust replacement model and remove no individual point. Visual and numerical exploratory summaries complement one another without converting this finite record into a random sample (Tukey, 1977).

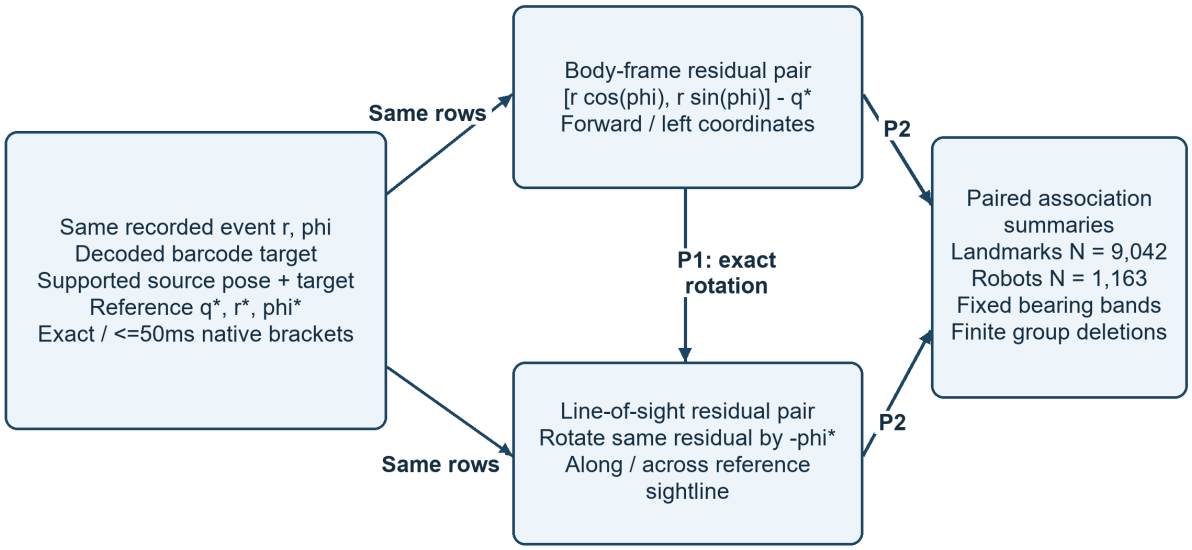

Figure 1. Research measurement model. P1 is the checked exact coordinate relationship. P2 compares actual association on the same supported rows and fixed bearing strata. The arrows represent calculations, not physical causal effects. Target classes and unsupported observations remain separate.

4. Actual support and joint relationships

The time and correspondence rules support 9,042 of 9,121 landmark events and 1,163 of 2,476 robot-target events. Another 1,259 events target robots 4-5, whose complete pose members are unavailable. There are 89 observer-gap exclusions, five target-gap exclusions, 39 target-coverage exclusions and the three unmapped codes. These mutually exclusive reasons account for all 11,600 rows. All 45 observer-landmark cells have support, ranging from 32 to 497 events. Observer 1 has a shorter reference record of 771.873 seconds; observers 2 and 3 cover 900 seconds. We preserve these unequal exposures rather than imply a balanced team experiment.

Table 1 answers the overall association question. Landmark residuals have a small positive polar Pearson correlation but a negative body correlation and positive sightline correlation. The body-minus-sightline contrast is -0.380587. Robot-target residuals have markedly different Pearson signs across the two Cartesian representations, giving a contrast of 1.660629. These are empirical features of the actual supported observations, including their association concerns. They are not evidence that rotating coordinates improves the measurements.

Table 1. Same-event Pearson residual associations, centered empirical summaries. N counts supported events, not independent experiments. Body x/y and along/across correlations use residual components in meters; polar correlation uses meters and wrapped radians. No calibration or estimator is fitted.

Target class	N	Behind-reference flags	Pearson r: range/angle	Pearson r: body x/y	Pearson r: along/across	Delta r: body-LOS
Static landmark	9042	4	0.0664	-0.2465	0.1341	-0.3806
Moving robot	1163	3	-0.5565	0.7898	-0.8708	1.6606

The covariance entries in Table 2 show the numerical scales behind those standardized coefficients. Body and sightline covariances are in square meters. The mixed-unit polar matrix is retained separately in the structured results and is not compared through eigenvalues with these Cartesian matrices. A change of sign in covariance or correlation is compatible with the exact vector relationship; it does not identify a different physical error for the same detection.

Table 2. Actual centered Cartesian residual covariance summaries, denominator N-1. First/second components mean forward/left for body coordinates and along/across for sightline coordinates. These matrices are empirical residual dispersion, not certified instrument uncertainty.

Target class	Coordinates	N	First variance (m²)	Second variance (m²)	Covariance (m²)
landmark	body	9042	0.044209	0.009770	-0.005123
landmark	los	9042	0.050897	0.002135	0.001398
robot	body	1163	0.148006	0.008083	0.027319
robot	los	1163	0.148909	0.008702	-0.031345

All observer-deletion and target-deletion contrasts are defined. For landmarks, their ranges remain negative under both complete deletion menus. For robot targets, both ranges span zero and extend to large positive values. Thus the positive full-record robot contrast cannot be presented as a stable direction across the observed composition checks. The menus and retained denominators are shown in Table 3; none is selected as a preferred corrected result.

Table 3. Finite group-deletion ranges for Delta r=body Pearson-LOS Pearson. Full N is 9,042 for landmarks and 1,163 for robot targets. Ranges include every declared observer/target deletion and are not confidence intervals.

Target class	Entire omitted group	Deletions	Retained N range	Delta r deletion range; not CI
landmark	observer	3	4723-7531	[-0.4227, -0.1364]
landmark	target	15	8002-8830	[-0.4115, -0.2770]
robot	observer	3	561-995	[-0.3452, 1.7599]
robot	target	3	562-910	[-0.3209, 1.8586]

The fixed angular strata also have different relationships (Table 4 and Figure 2). In the landmark left band, body correlation is -0.7982 while sightline correlation is 0.3468; the center-band values are 0.3731 and 0.3216. For robot targets, the right band gives 0.8877 versus 0.2822. These differences show what pooled coefficients conceal. They are conditional descriptions of different recorded geometry and target composition, rather than estimates of a causal response to changing bearing.

Table 4. Pearson relationships in all six class×reference-bearing strata. Left phi∗<-0.20 rad; center-0.20≤phi∗≤0.20 rad; right phi∗>0.20 rad. Outer strata retain flagged observations. The observer-specific 18 cells are also saved without discarding sparse support.

Target class	Reference-bearing band	N	Flags	Body Pearson r	LOS Pearson r	Delta r
landmark	left	2494	0	-0.7982	0.3468	-1.1450
landmark	center	3777	0	0.3731	0.3216	0.0516
landmark	right	2771	4	-0.3334	-0.2355	-0.0980
robot	left	326	3	0.8619	-0.9656	1.8275
robot	center	491	0	0.3847	0.3603	0.0243
robot	right	346	0	0.8877	0.2822	0.6055

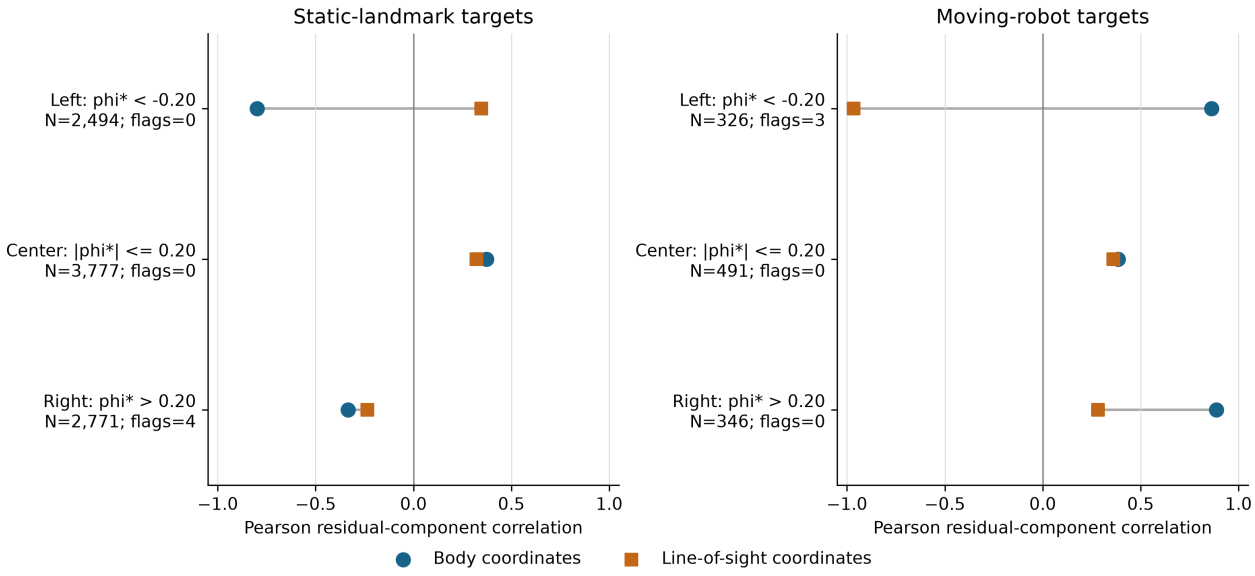

Figure 2. Same-row body and sightline Pearson coefficients by target class and fixed reference-bearing band. Connectors pair two summaries; they are not fitted trends or intervals. N and behind-reference flag counts are stated for every band.

5. What rank association and reference checks add

Pearson coefficients do not tell the whole association story. Landmark body and sightline Spearman correlations are 0.1849 and 0.4519, respectively, compared with Pearson values -0.2465 and 0.1341. For robot targets, the Spearman values are 0.1733 and 0.4390, while polar Spearman correlation is 0.4053. The corresponding robot polar Pearson coefficient is -0.5565. All rows remain in both summaries. These discrepancies preclude treating a single linear coefficient as a complete description of dependence, and rank correlation itself is not an independence test.

Seven supported records place their assigned target behind the observer in the source-reference geometry, although their measured bearings are front-facing. Four are observer 3 landmark-subject 20 rows 1509, 1513, 1517 and 1521; three are robot-subject 2 rows 3750, 3753 and 3757. Their raw IDs and timestamps remain available. The original source warns that partial barcode occlusion can produce incorrect identifiers. That is a possible explanation, not an adjudicated correction here. We neither relabel these targets nor discard them because of a large residual. Consequently, the reported matrices include association ambiguity alongside other discrepancies.

This matters especially for interpreting strong robot-target Pearson coefficients. Two of the three flagged robot events have exact-native observer timestamps. A reference with no observer interpolation can still participate in a questionable correspondence. More generally, measurement error in variables and reference information can alter observed relationships; a derived reference is not an independent error-free covariate (Carroll et al., 2006). Our analysis cannot attribute the entire body/sightline contrast to camera-channel coupling, and it does not establish which part originates in the reference or the correspondence.

The limited exact-native check contains 544 landmark and 79 robot observations, requiring exact native timestamps for every moving pose involved. Landmark body and sightline correlations become 0.1662 and 0.4193. The robot values are 0.9699 and -0.9848, with two flagged observations still present. The subset differs in geometry and composition as well as interpolation. It therefore cannot identify the causal contribution of interpolation, nor does it certify a cleaner population or a physically exact measurement. It supplies the declared conditional check and its actual denominator.

6. Implications and reproducible scope

The practical implication is to report a correlation together with its residual definition, axes, target class and support. A body-coordinate coefficient cannot be substituted for an along/across coefficient merely because both arise from the same range-bearing pair. Nor can a near-zero polar Pearson coefficient demonstrate independent sensing channels when rank association, angular mixture and correspondence flags provide different information. The experiment here is a retrospective accounting of that information, with no newly controlled bearing, noise injection, calibration fit or localization trial.

The nonlinear Cartesian conversion and event-specific sightline rotation are familiar mathematical operations. What the released data add are the measured coefficient values, their angular strata, and their sensitivity to complete observer/target deletions. In particular, the landmark contrast remains negative throughout the specified deletion menus while the robot contrast changes direction. This distinction concerns the available target populations. It is not a ranking of static and moving sensing quality, because their range distributions, visibility, observer exposure and reference requirements differ.

Several limitations constrain generalization. The source is one recording with three available observers, not a designed collection of independent operating runs. Interpolation gaps are bounded but approximation remains, NTP performance is documented rather than independently measured, and

missing target poses restrict which robot events are evaluable. Shared camera processing, source pose errors and association ambiguity cannot be separated into physical noise components by these summaries. The bands are fixed descriptive partitions and their outer tails are deliberately retained. The study supplies neither a Gaussian likelihood nor a covariance choice validated in a downstream filter.

The saved record includes member identity checks, an integer-clock support table containing every raw row, the frozen protocol, full covariance/rank summaries, all 24 group deletions, figures and actual-byte output hashes. A separate raw-text checker advances through native timestamps without importing the primary lookup and uses independent scalar coordinate formulas, compensated sums and hand-computed average ranks. It checks all 11,600 rows, 34 summary groups and 24 deletions, with maximum independent scalar geometry difference 2.6e-15 m. All support and group definitions match exactly. Numerical agreement establishes reproducibility of this calculation, not replication of sensing conditions; that distinction is consistent with computational reproducibility principles (Peng, 2011).

Keeping the original and processed records distinct follows practical reproducible-computation guidance (Sandve et al., 2013; Wilson et al., 2017). Provenance and clear usage conditions also support reusable data (Wilkinson et al., 2016). The institution makes the dataset publicly available for research and requests attribution; no named unconditional redistribution licence was found. We do not redistribute the original archive or substitute a code licence for data terms.

The supported MR.CLAM observations demonstrate substantial empirical coordinate dependence, with different conclusions from linear and rank association and different stability across target classes. Preserving identity, timing support and exceptional geometry is necessary to interpret those results. An axis-specific residual coefficient is a description of a defined record and representation, not a stand-alone property of an instrument or a controller.

References

1. Spearman, C.. (1904). The Proof and Measurement of Association between Two Things. The American Journal of Psychology. https://doi.org/10.2307/1412159
2. Wilson, Greg; Bryan, Jennifer; Cranston, Karen; Kitzes, Justin; Nederbragt, Lex; Teal, Tracy K.. (2017). Good enough practices in scientific computing. PLOS Computational Biology. https://doi.org/10.1371/journal.pcbi.1005510
3. Sandve, Geir Kjetil; Nekrutenko, Anton; Taylor, James; Hovig, Eivind. (2013). Ten Simple Rules for Reproducible Computational Research. PLoS Computational Biology. https://doi.org/10.1371/journal.pcbi.1003285
4. Lynch, Kevin M.; Park, Frank C.. (2017). Modern Robotics: Mechanics, Planning, and Control. Cambridge University Press. https://doi.org/10.1017/9781316661239
5. Wilkinson, Mark D.; Dumontier, Michel; Aalbersberg, IJsbrand Jan; Appleton, Gabrielle; Axton, Myles; Baak, Arie; Blomberg, Niklas; Boiten, Jan-Willem; da Silva Santos, Luiz Bonino; Bourne, Philip E.; Bouwman, Jildau; Brookes, Anthony J.; Clark, Tim; Crosas, Mercè; Dillo, Ingrid; Dumon, Olivier; Edmunds, Scott; Evelo, Chris T.; Finkers, Richard; Gonzalez-Beltran, Alejandra; Gray, Alasdair J.G.; Groth, Paul; Goble, Carole; Grethe, Jeffrey S.; Heringa, Jaap; 't Hoen, Peter A.C; Hooft, Rob; Kuhn, Tobias; Kok, Ruben; Kok, Joost; Lusher, Scott J.; Martone, Maryann E.; Mons, Albert; Packer, Abel L.; Persson, Bengt; Rocca-Serra, Philippe; Roos, Marco; van Schaik, Rene; Sansone, Susanna-Assunta; Schultes, Erik; Sengstag, Thierry; Slater, Ted; Strawn, George; Swertz, Morris A.; Thompson, Mark; van der Lei, Johan; van Mulligen, Erik; Velterop, Jan; Waagmeester, Andra; Wittenburg, Peter; Wolstencroft, Katherine; Zhao, Jun; Mons, Barend. (2016). The FAIR Guiding Principles for scientific data management and stewardship. Scientific Data. https://doi.org/10.1038/sdata.2016.18
6. Gebru, Timnit; Morgenstern, Jamie; Vecchione, Briana; Vaughan, Jennifer Wortman; Wallach, Hanna; Daumé III, Hal; Crawford, Kate. (2021). Datasheets for datasets. Communications of the ACM. https://doi.org/10.1145/3458723
7. Mardia, Kanti V.; Jupp, Peter E.. (1999). Directional Statistics. Wiley Series in Probability and Statistics. https://doi.org/10.1002/9780470316979
8. Kendall, Maurice G.. (1945). THE TREATMENT OF TIES IN RANKING PROBLEMS. Biometrika. https://doi.org/10.1093/biomet/33.3.239

9. Lerro, D.; Bar-Shalom, Y.. (1993). Tracking with debiased consistent converted measurements versus EKF. IEEE Transactions on Aerospace and Electronic Systems. https://doi.org/10.1109/7.220948

10. Peng, Roger D. (2011). Reproducible Research in Computational Science. Science. https://doi.org/10.1126/science.1213847

11. Huber, Peter J.; Ronchetti, Elvezio M.. (2009). Robust Statistics. Wiley Series in Probability and Statistics. https://doi.org/10.1002/9780470434697

12. Goldberg, David. (1991). What every computer scientist should know about floating-point arithmetic. ACM Computing Surveys. https://doi.org/10.1145/103162.103163

13. Bar-Shalom, Yaakov; Li, X. Rong; Kirubarajan, Thiagalingam. (2001). Estimation with Applications to Tracking and Navigation: Theory, Algorithms and Software. Wiley. https://doi.org/10.1002/0471221279

14. Hampel, Frank R.. (1974). The Influence Curve and its Role in Robust Estimation. Journal of the American Statistical Association. https://doi.org/10.1080/01621459.1974.10482962.

15. Xu, Dan; Guo, Yunxiao; Yu, Zhongyi; Wang, Zhenfeng; Lan, Rongze; Zhao, Runhao; Xie, Xinjia; Long, Han. (2023). PPO-Exp: Keeping Fixed-Wing UAV Formation with Deep Reinforcement Learning. Drones. https://doi.org/10.3390/drones7010028

16. Carroll, Raymond J.; Ruppert, David; Stefanski, Leonard A.; Crainiceanu, Ciprian M.. (2006). Measurement Error in Nonlinear Models. Chapman and Hall/CRC. https://doi.org/10.1201/9781420010138

17. Pearson, Karl. (1896). VII. Mathematical contributions to the theory of evolution.-III. Regression, heredity, and panmixia. Philosophical Transactions of the Royal Society of London. Series A, Containing Papers of a Mathematical or Physical Character. https://doi.org/10.1098/rsta.1896.0007

18. Wang, Richard Y.; Strong, Diane M.. (1996). Beyond Accuracy: What Data Quality Means to Data Consumers. Journal of Management Information Systems. https://doi.org/10.1080/07421222.1996.11518099

19. Fisher, N. I.. (1993). Statistical Analysis of Circular Data. Cambridge University Press. https://doi.org/10.1017/cbo9780511564345

20. Thrun, Sebastian; Burgard, Wolfram; Fox, Dieter. (2005). Probabilistic Robotics. MIT Press. ISBN9780262201629. https://mitpress.mit.edu/9780262201629/probabilistic-robotics/

21. Julier, Simon J.; Uhlmann, Jeffrey K.; Durrant-Whyte, Hugh F.. (2000). A new method for the nonlinear transformation of means and covariances in filters and estimators. IEEE Transactions on Automatic Control. https://doi.org/10.1109/9.847726

22. Joint Committee for Guides in Metrology. (2011). Evaluation of measurement data - Supplement 2 to the Guide to the expression of uncertainty in measurement - Extension to any number of output quantities (JCGM 102:2011). BIPM. https://www.bipm.org/documents/20126/2071204/JCGM_102_2011_E.pdf

23. Sullivan, Nick; Grainger, Steven; Cazzolato, Ben. (2018). Analysis of cooperative localisation performance under varying sensor qualities and communication rates. Robotics and Autonomous Systems. https://doi.org/10.1016/j.robot.2018.09.010

24. Barfoot, Timothy D.. (2017). State Estimation for Robotics. Cambridge University Press. https://doi.org/10.1017/9781316671528

25. Joint Committee for Guides in Metrology. (2008). Evaluation of measurement data - Guide to the expression of uncertainty in measurement (JCGM100:2008). BIPM. https://www.bipm.org/documents/20126/2071204/JCGM_100_2008_E.pdf

26. Autonomous Space Robotics Lab. (n.d.). UTIAS Multi-Robot Cooperative Localization and Mapping Dataset: file format, reference frames and access tools. University of Toronto Institute for Aerospace Studies. https://asrl.utias.utoronto.ca/datasets/mrclam/

27. Higham, Nicholas J.. (2002). Accuracy and Stability of Numerical Algorithms: Second Edition. Society for Industrial and Applied Mathematics. https://doi.org/10.1137/1.9780898718027

28. Leung, Keith YK; Halpern, Yoni; Barfoot, Timothy D; Liu, Hugh HT. (2011). The UTIAS multi-robot cooperative localization and mapping dataset. The International Journal of Robotics Research. https://doi.org/10.1177/0278364911398404

29. Julier, Simon J.; Uhlmann, Jeffrey K.. (2004). Unscented Filtering and Nonlinear Estimation. Proceedings of the IEEE. https://doi.org/10.1109/jproc.2003.823141

30. Tukey, John W.. (1977). Exploratory Data Analysis. Addison-Wesley. https://www.pearson.com/en-us/subject-catalog/p/exploratory-data-analysis-classic-version-/P200000006400